NACA

RESEARCH MEMORANDUM

LARGE-SCALE LOW-SPEED WIND-TUNNEL TESTS OF A MODEL HAVING A 60° DELTA HORIZONTAL CANARD CONTROL SURFACE AND WING TO OBTAIN STATIC-LONGITUDINAL-STABILITY AND CANARD-SURFACE HINGE-MOMENT DATA

By Dale L. Burrows

Langley Aeronautical Laboratory
Langley Field, Va.

CLASSIFIED DOCUMENT

NATIONAL ADVISORY COMMITTEE
FOR AERONAUTICS

WASHINGTON
June 17, 1954

Classification cancelled (or changed to Unclassified)

By Authority of Nasa Tech Pub Announcement #99
(OFFICER AUTHORIZED TO CHANGE)

By 13 Apr 66

NC
(GRADE OF OFFICER MAKING CHANGE)

6 April 61
DATE

[redacted]

NATIONAL ADVISORY COMMITTEE FOR AERONAUTICS

RESEARCH MEMORANDUM

LARGE-SCALE LOW-SPEED WIND-TUNNEL TESTS OF A MODEL HAVING A 60° DELTA HORIZONTAL CANARD CONTROL SURFACE AND WING TO OBTAIN STATIC-LONGITUDINAL-STABILITY AND CANARD-SURFACE HINGE-MOMENT DATA

By Dale L. Burrows

SUMMARY

A wind-tunnel investigation was made of a model equipped with a 60° delta wing and a 60° delta horizontal all-movable canard control surface to determine the stability, control, and canard-surface hinge-moment characteristics at low speeds and at a Reynolds number of 9×10^6. Two longitudinal positions of the canard surface were tested. Data of lift, drag, pitching moments, and canard-surface hinge moments are presented through an angle-of-attack range of -10° to 45° and a canard-surface deflection range of -5° to 20°.

The results indicated that adding a tail at zero incidence had no appreciable effect on the lift-curve slope near zero angle of attack. At higher angles of attack, the canard surface increased the lift-curve slope until at 25° the increased lift was proportional to increased lifting area. With either tail length and with canard-surface deflection angles of zero and greater, the canard surface approached stall at angles of attack which were lower than those for wing stall. For two reasonable values of the static margin differing by about 0.06 of the mean aerodynamic chord, the maximum trim lift coefficient changed from about 1.4 to 1.0.

Values of the rate of change of canard-surface hinge-moment coefficient with angle of attack and canard-surface deflection angle for either tail-length configuration were negative only through a small range of angles near zero and were markedly positive at higher angles.

[redacted]

[redacted]

INTRODUCTION

Interest in the canard-type of aircraft continues because of possible high-speed advantages in stability and control over the conventional type of aircraft. The merits of canard configurations have been analyzed in reference 1 and a considerable amount of research has been conducted on various canard configurations (for example, refs. 2 to 7). As a result of such research, it is generally recognized that there are problems with the canard configuration at low speeds and in particular there is a lack of stability and control data at large-scale Reynolds numbers. Also there are few data available on hinge moments for canard control surfaces at low speeds. Reference 8 presents canard-surface hinge moments for a Mach number range from 0.8 to 2.0.

The purpose of the present investigation was to obtain longitudinal stability and control data and in particular horizontal-tail hinge moments for a canard configuration at low speeds and large values of the Reynolds number. The tests were conducted in the Langley low-turbulence pressure tunnel on a model having a 60° delta all-movable horizontal canard surface and a 60° delta wing mounted on a sharp-nosed, blunt-based body of revolution having a fineness ratio of 10.

Measurements were made of the model normal force, chord force, and pitching moments and horizontal-canard-surface hinge moments for two longitudinal locations of the canard surface at a Mach number of about 0.15 and a Reynolds number of 9×10^6 based on the mean aerodynamic chord of the wing. The angle of attack was varied through a range from about -10° to 45° and the canard surface was deflected through a range of angles from -5° to 20°.

Downwash surveys of this canard configuration were reported in reference 9 for a similar range of angles of attack and for zero canard-surface deflection.

SYMBOLS

The coordinate system used and the directions of positive forces, moments, and angles are shown in figure 1.

C_N normal-force coefficient, Normal force/qS_w

C_X longitudinal-force coefficient, Longitudinal force/qS_w

C_m pitching-moment coefficient about a point $0.29\bar{c}_w$ ahead of $\bar{c}_w/4$, Pitching moment/$qS_w\bar{c}_w$

C_L lift coefficient, $C_X \sin \alpha + C_N \cos \alpha$

$C_{L_{trim}}$ lift coefficient at zero pitching-moment coefficient

C_D drag coefficient, $-C_X \cos \alpha + C_N \sin \alpha$

C_h canard-surface hinge-moment coefficient, Hinge moment/$qS_t\bar{c}_t$

C_{h_α} partial rate of change of hinge-moment coefficient with angle of attack

C_{h_δ} partial rate of change of hinge-moment coefficient with canard-surface deflection angle

b_t total span of canard surface

b_w total span of wing

c_t local chord length of canard surface

c_w local chord length of wing

$\bar{c}_t$ canard-surface mean aerodynamic chord, $\frac{2}{S_t}\int_0^{b_t/2} c_t^2 db_t$

$\bar{c}_w$ wing mean aerodynamic chord, $\frac{2}{S_w}\int_0^{b_w/2} c_w^2 db_w$

q free-stream dynamic pressure, $\frac{1}{2}\rho U^2$

S_t canard-surface plan-form area, $2\int_0^{b_t/2} c_t db_t$

S_w wing plan-form area, $2\int_0^{b_w/2} c_w db_w$

U free-stream velocity

[redacted]

α angle of attack of fuselage

δ_t angle of incidence of canard surface with respect to body axis

ρ free-stream mass density

MODEL AND APPARATUS

The model for this investigation had a canard horizontal control surface and a wing surface both of 60° delta plan form and NACA 65A006 airfoil section parallel to the plane of symmetry. The wing was mounted in a midfuselage position and at zero incidence with respect to the fuselage center line (see fig. 2).

The wing had a mean aerodynamic chord of 10.53 inches and an area five times the area of the control surface. The $\bar{c}_w/4$ station on the wing was located at $2.18\bar{c}_w$ behind the body nose. The wing trailing edge was located $0.23\bar{c}_w$ ahead of the base of the body.

The coordinates of the pointed body of revolution of fineness ratio 10 were the same as for the closed body of fineness ratio 12 described in reference 10. The lower fineness ratio was obtained for this investigation by removing the pointed tail of the basic body. The resulting body length was 316 percent of the wing mean aerodynamic chord.

The mean aerodynamic chord of the all-movable canard surface was 4.70 inches and the hinge line was at $0.32\bar{c}_t$. The two longitudinal positions of the canard surface were obtained by moving the canard surface with respect to the wing and body. For the long- and short-tail-length configurations, the $\bar{c}_t/4$ positions were $1.73\bar{c}_w$ and $1.44\bar{c}_w$ ahead of the pitch axis. The apexes of the canard surfaces for the long and short tail length were $0.17\bar{c}_w$ ahead and $0.12\bar{c}_w$ behind the leading point of the basic body. The canard surface could be adjusted in pitch through an angle range of ±20° with respect to the body axis. At a canard-surface deflection of zero, a minimum gap of about 0.02 inch existed between the body and canard surface aft of the hinge. This gap, which increased with canard-surface deflection, was not sealed for any of the tests. The nose section of the body forward of the hinge pivoted with the canard surface. The surface discontinuity at the ball pivot joint was not faired for any of the tests.

The tests were conducted in the Langley low-turbulence pressure tunnel described in reference 11. The model was sting mounted in the tunnel. The model forces and moments were measured by an internal six-component strain-gage balance, whose pitch axis was located at $0.29\bar{c}_w$

ahead of $\bar{c}_w/4$. An additional strain-gage balance was located internally on the canard-surface hinge line to measure hinge moments. Static-pressure tubes on the sides of the sting and inside of the model base were used for measuring base pressures.

TESTS

The air in the wind tunnel during the tests was compressed to 150 lb/sq in. abs to obtain a constant Reynolds number of 9×10^6 (based on the mean aerodynamic chord of the wing) at a constant Mach number of 0.15. The angle of attack was varied through a range of about -10° to 45° in combination with a variation in canard-surface deflection through an angle range of -5° to 20°. All of the tests were for zero sideslip angle.

For both cases of canard surface off and on, measurements were made of the chord forces, normal forces, base pressures, and the pitching moments about a point $0.29\bar{c}_w$ ahead of $\bar{c}_w/4$. Canard-surface hinge moments were also measured.

CORRECTIONS

The usual tunnel blocking corrections described in reference 12 were applied to all force and moment coefficients and pressure data. The angle of attack was corrected for model-support deflection due to aerodynamic loading and was also corrected for tunnel induced upwash by the method of reference 13. The differences in induced upwash angles at the wing and canard surface were also taken into account. The correction to canard-surface angle of incidence for canard-surface deflection due to aerodynamic loading was negligibly small.

The longitudinal-force data which included the pressure force on the base were adjusted to make the base pressure equal to the free-stream static pressure.

RESULTS AND DISCUSSION

Lift and drag coefficients were obtained from the measured chord and normal forces by the relations shown in the list of symbols. The lift coefficients are plotted against angle of attack and pitching moment in figure 3(a) for the short tail length and in figure 3(b) for the long tail length. The pitching moments are also plotted against

angle of attack in figure 3(a) for the short tail length and in figure 3(b) for the long tail length. Trim lift coefficients for the two tail lengths and two values of static margin are plotted in figure 4 against canard-surface deflection angle. The center-of-gravity positions for the two values of the static margin are shown in a sketch in figure 5. Drag-lift polars are presented in figures 6(a) and 6(b) to two different scales to clarify high and low angle-of-attack ranges. Canard-surface hinge moments are plotted against α for constant values of δ_t in figure 7 and against δ_t for constant values of α in figure 8.

Lift and Pitching Moment

For either the short or long tail length (figs. 3(a) and 3(b)), adding the canard surface at zero deflection angle did not appreciably increase the lift-curve slope of the wing and body alone near zero angle of attack in spite of the increase in lifting-surface area which amounted to 0.20 of the wing area. This effect is probably the result of canard-surface downwash which reduced the effective angle of attack of the wing. At angles of attack of about 4° and higher, the lift-curve slope of the canard surface together with the wing-body combination increases over that of the wing-body combination alone until at an angle of attack of 25° the lifts for canard surface off and canard surface on are in proportion to the increased lifting-surface area.

Increasing the canard-surface deflection angle caused an increased nonlinearity of the lift-curve slope at low angles of attack. This latter effect was probably caused by the wing passing through the canard-surface trailing vortex and to some extent by the effect of the canard-surface—body gap. Addition of the canard surface produced a marked decrease in stability at all angles of attack below stall with the longer tail length producing the greatest change which resulted in nearly neutral stability at the low angles of attack. The increased stability at moderate angles of attack over that at low angles indicates that for all positive deflections the canard surface stalls at lower angles of attack than those at which the wing stalls. As would be expected, the angle of attack at which this increase in stability occurs decreases with increasing canard-surface deflection.

A plot of trim lift coefficient against canard-surface deflection angle is shown in figure 4 for two degrees of longitudinal stability corresponding to two values of the zero-lift static margin (the distance between the center of gravity and the zero-lift neutral point). One static margin was chosen as the minimum required for neutral stability at some trim condition and positive stability at all others. The other more stable static margin was used to indicate the effects of a change in stability on the trim-lift characteristics.

With an increase in static margin of $0.062\bar{c}$, the maximum trim lift coefficient changes from about 1.4 to 1.0 for the short tail length and from about 1.3 to 1.05 for the long tail length. The maximum lift coefficient of the configuration without a canard surface and therefore untrimmed was 1.17. Throughout the trim-lift range for the static margins chosen, the model was stable and had no large or abrupt changes in stability.

Through most of the canard-surface deflection range the changes in trim lift coefficient for a given change in static margin are smaller for the long-tail-length configuration. Also the rate of change of trim lift coefficient with canard-surface deflection angle is smaller for the longer tail length in the unstalled region.

A sketch of the center-of-gravity positions required for the two values of static margin considered is shown in figure 5 for the two tail lengths. In general, these center-of-gravity positions are forward of or in the vicinity of the leading edge of the mean aerodynamic chord and, as would be expected for equal static margins, the longer tail length requires a center-of-gravity position forward of that for the short tail length.

Drag

Adding the canard surface at zero incidence for either tail-length position increased the drag coefficient by about 0.0015 at zero lift as shown in figure 6. Above a lift coefficient of 0.45, adding the canard surface at zero incidence reduced the drag coefficient of the wing-fuselage combination.

Hinge Moment

Values of the canard-surface hinge-moment coefficients about $0.35\bar{c}_t$ for the two tail lengths are shown in figure 7 plotted against angle of attack for various surface deflection angles and are cross-plotted in figure 8 for several angles of attack. As may be seen from figures 7 and 8, values of C_{h_α} and C_{h_δ} near $\alpha = \delta = 0$ are negative and are slightly larger for the short tail length than for the long tail length. For moderate increases in α and δ_t, however, the values of C_{h_α} and C_{h_δ} become positive and do so at larger values of α and δ_t for the short tail length than for the long tail length. These apparent effects of tail length are probably due to some differences in exposed canard-surface area and differences in interference of the various components on the canard surface, such as canard-surface—body gap, model nose, and possibly the wing itself. While there are rather sudden negative breaks in C_{h_α} and C_{h} [redacted] combinations of angle of attack and

canard-surface deflection angles that sum to about 40°, examination of figures 3 and 4 will indicate that such a combination of angles is outside of the trim range for the static margins considered.

CONCLUSIONS

A wind-tunnel investigation of a model equipped with a 60° delta wing and a 60° delta horizontal canard control surface at two tail lengths to determine the stability, control, and tail hinge-moment characteristics at low speeds and at a Reynolds number of 9×10^6 has led to the following conclusions:

1. Adding the canard surface at zero deflection and at either the long or short tail length had no appreciable effect on the lift-curve slope near zero angle of attack but increased the lift-curve slope at higher angles of attack, until at 25° the increased lift was proportional to increased lifting area.

2. For either the long- or short-tail-length configuration at zero or positive deflection, the canard surface stalled at angles of attack lower than that for wing stall.

3. For two reasonable values of the static margin differing by about 0.06 of the mean aerodynamic chord, the maximum trim lift coefficient changed from about 1.4 to 1.0 with increasing static margin. Throughout the trim-lift range for the static margins chosen, the model was longitudinally stable and had no large or abrupt changes in longitudinal stability.

4. The rates of change of trim lift coefficient with static margin or with canard-surface deflection angle were smaller for the longer tail length.

5. In general, for both tail lengths and for the particular hinge positions used, the values of the rate of change of canard-surface hinge-moment coefficient with angle of attack and deflection angle were negative through a small range of angles near zero but changed markedly positive for slightly higher angles of attack and deflection.

Langley Aeronautical Laboratory,
National Advisory Committee for Aeronautics,
Langley Field, Va., April 9, 1954.

REFERENCES

1. Mathews, Charles W.: Study of the Canard Configuration With Particular Reference to Transonic Flight Characteristics and Low-Speed Characteristics at High Lift. NACA RM L8G14, 1949.

2. Curfman, Howard J., Jr., and Grigsby, Carl E.: Longitudinal Stability and Control Characteristics of a Canard Missile Configuration for Mach Numbers From 1.1 to 1.93 as Determined From Free-Flight and Wind-Tunnel Investigations. NACA RM L52F06, 1952.

3. Stephenson, Jack D., and Selan, Ralph: The Static Longitudinal Characteristics at Mach Numbers up to 0.95 of a Triangular-Wing Canard Model Having a Triangular Control. NACA RM A51I07, 1951.

4. Niewald, Roy J., and Moul, Martin T.: The Longitudinal Stability, Control Effectiveness, and Control Hinge-Moment Characteristics Obtained From a Flight Investigation of a Canard Missile Configuration at Transonic and Supersonic Speeds. NACA RM L50I27, 1950.

5. Crane, Harold L., and Adams, James J.: Wing-Flow Measurements of Longitudinal Stability and Control Characteristics of a Canard Airplane Configuration With a 45° Sweptback Wing and a Triangular All-Movable Control Surface. NACA RM L50A31, 1950.

6. Johnson, Joseph L., Jr.: A Study of the Uses of Various High-Lift Devices on the Horizontal Tail of a Canard Airplane Model as a Means of Increasing the Allowable Center-of-Gravity Travel. NACA RM L52K18a, 1953.

7. Bates, William R.: Low-Speed Static Longitudinal Stability Characteristics of a Canard Model Having a 60° Triangular Wing and Horizontal Tail. NACA RM L9H17, 1949.

8. Brown, Clarence A., Jr., and Lundstrom, Reginald R.: Flight Investigation From Mach Number 0.8 to Mach Number 2.0 To Determine Some Effects of Wing-to-Tail Distance on the Longitudinal Stability and Control Characteristics of a 60° Delta-Wing—Canard Missile. NACA RM L52C26, 1952.

9. Newman, Ernest E., and Cahill, Jones F.: Investigation at Low Speed of the Flow Field Behind the Lifting Surfaces of a Model Equipped With a 60° Triangular Wing and a 60° Triangular Canard Tail. NACA RM L53C30, 1953.

[redacted]

10. Loving, Donald L., and Wornom, Dewey E.: Transonic Wind-Tunnel Investigation of the Interference Between a 45° Sweptback Wing and a Systematic Series of Four Bodies. NACA RM L52J01, 1952.

11. Von Doenhoff, Albert E., and Abbott, Frank T., Jr.: The Langley Two-Dimensional Low-Turbulence Pressure Tunnel. NACA TN 1283, 1947.

12. Herriot, John G.: Blockage Corrections for Three-Dimensional-Flow Closed-Throat Wind Tunnels, With Consideration of the Effect of Compressibility. NACA Rep. 995, 1950. (Supersedes NACA RM A7B28.)

13. Katzoff, S., and Hannah, Margery E.: Calculation of Tunnel-Induced Upwash Velocities for Swept and Yawed Wings. NACA TN 1748, 1948.

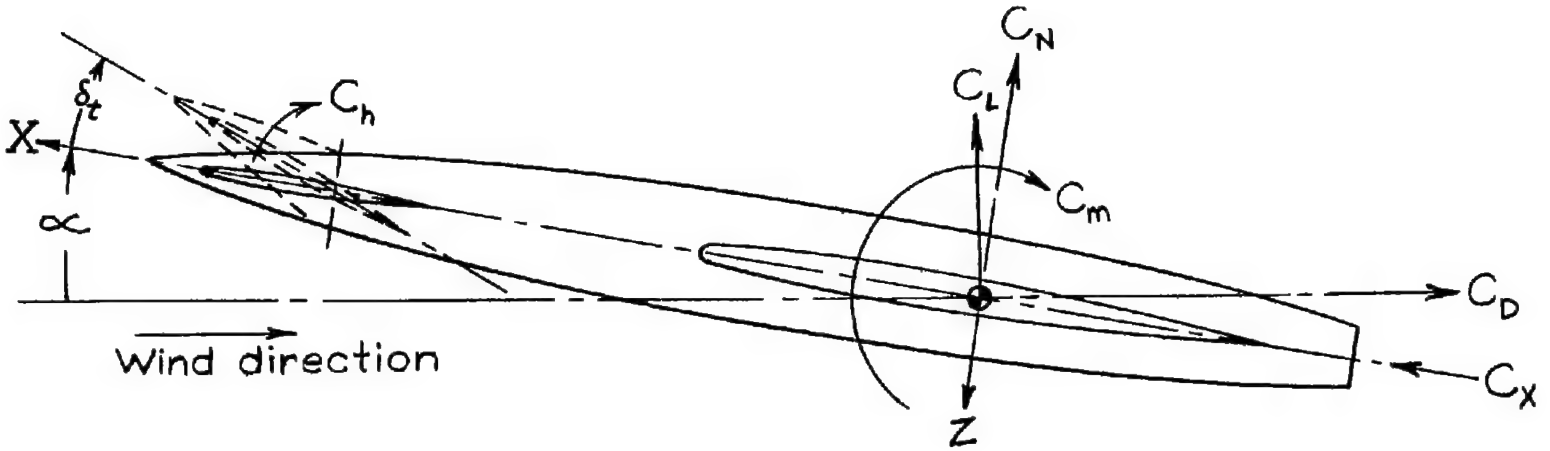

Figure 1.- The model system of axes. Arrows indicate positive directions of moments and forces.

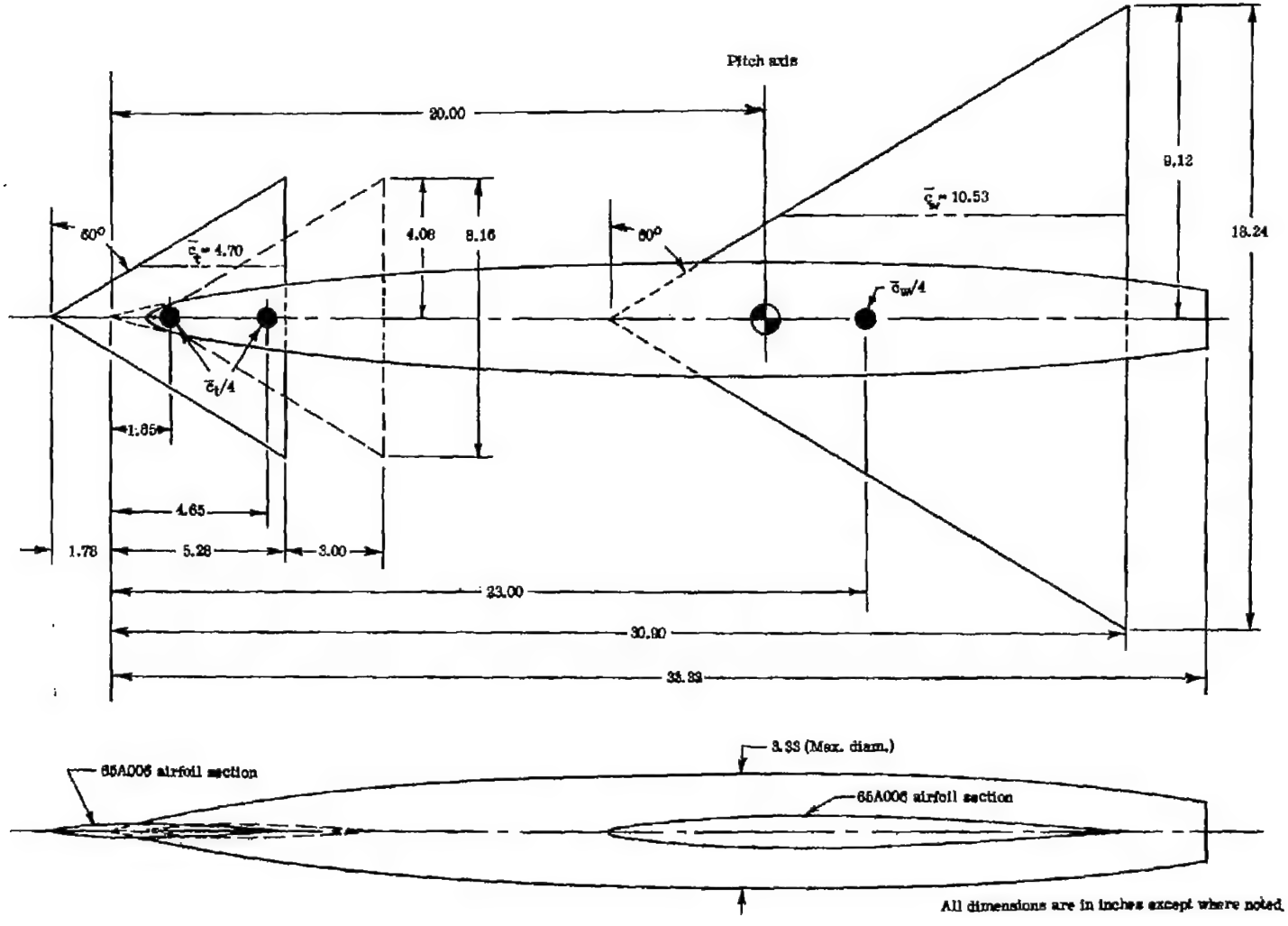

(a) General dimensions.

Figure 2.- Sketches of model.

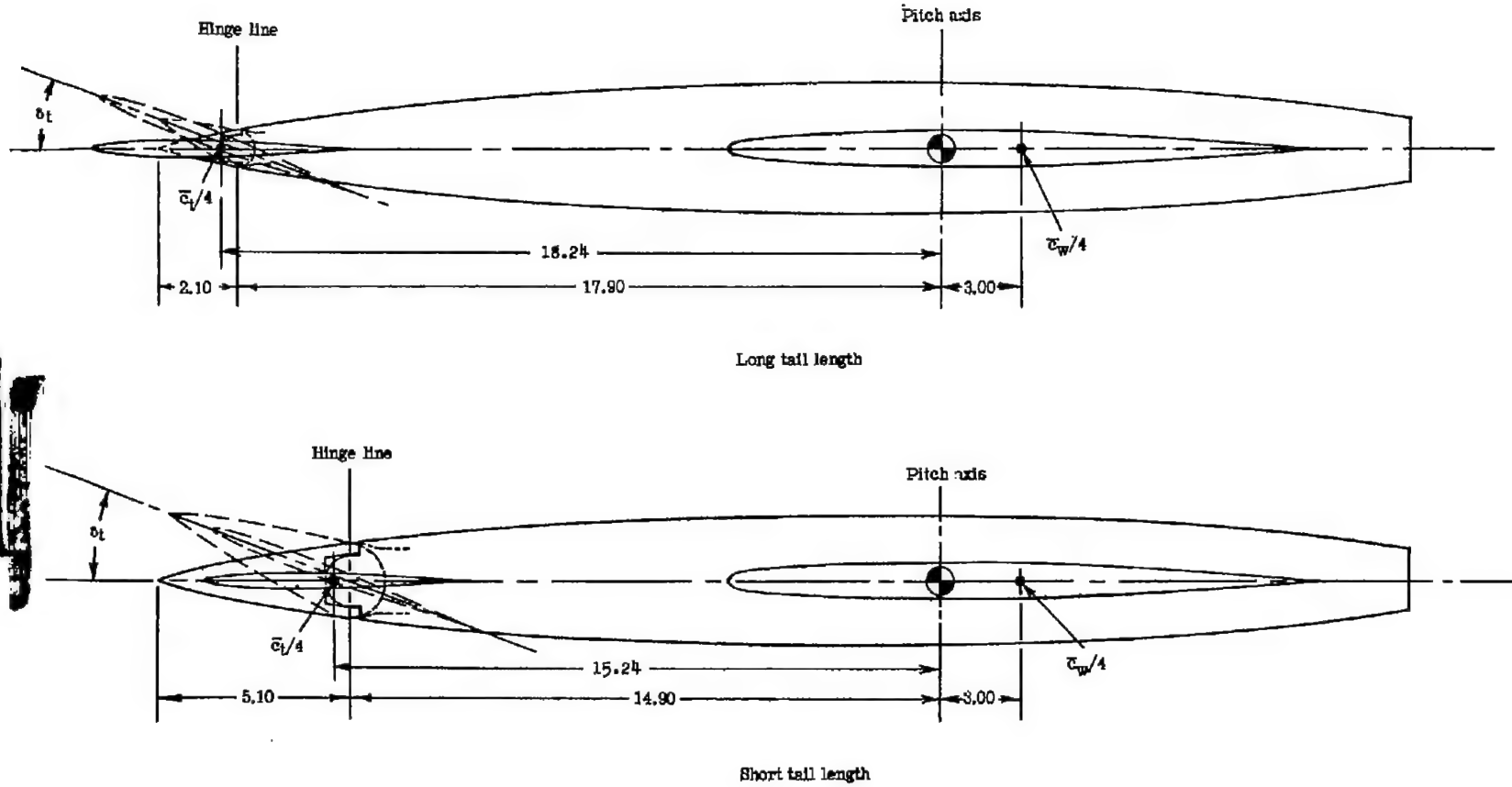

(b) Hinge detail.

Figure 2.- Concluded.

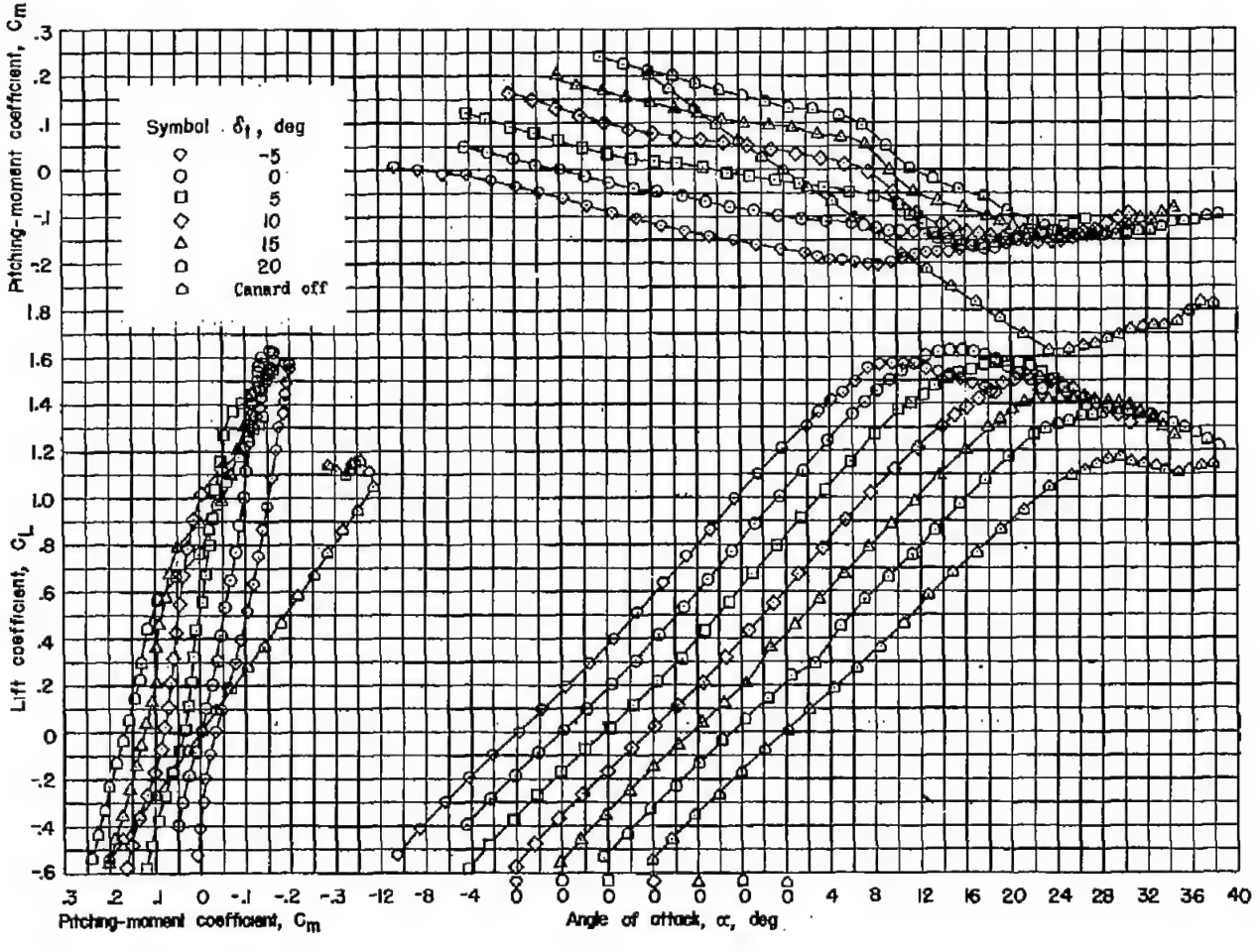

(a) Short tail length.

Figure 3.- Variation of lift and moment coefficients with angle of attack for a configuration having a wing and horizontal canard surface of 60° delta plan form.

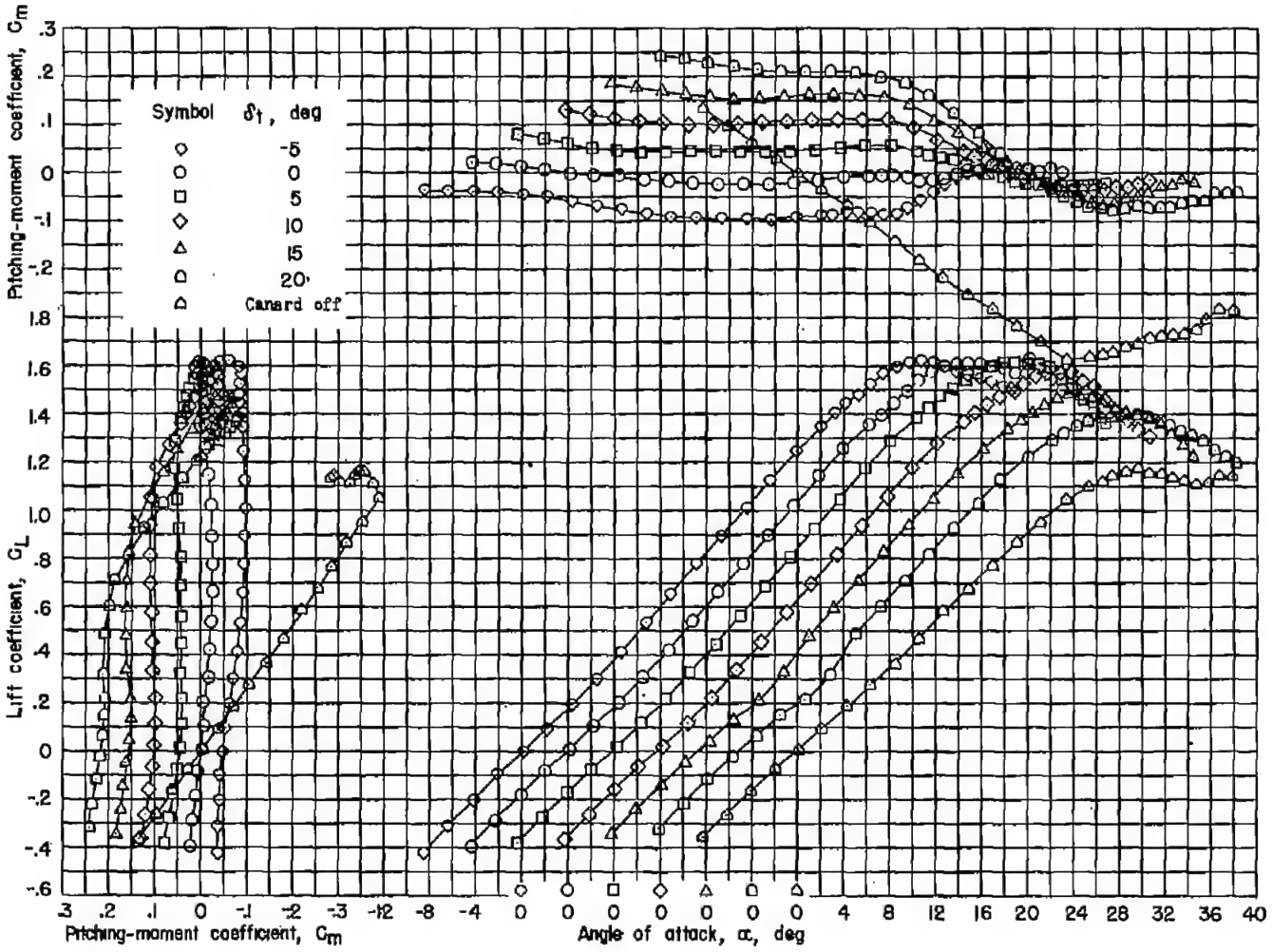

(b) Long tail length.

Figure 3.- Concluded.

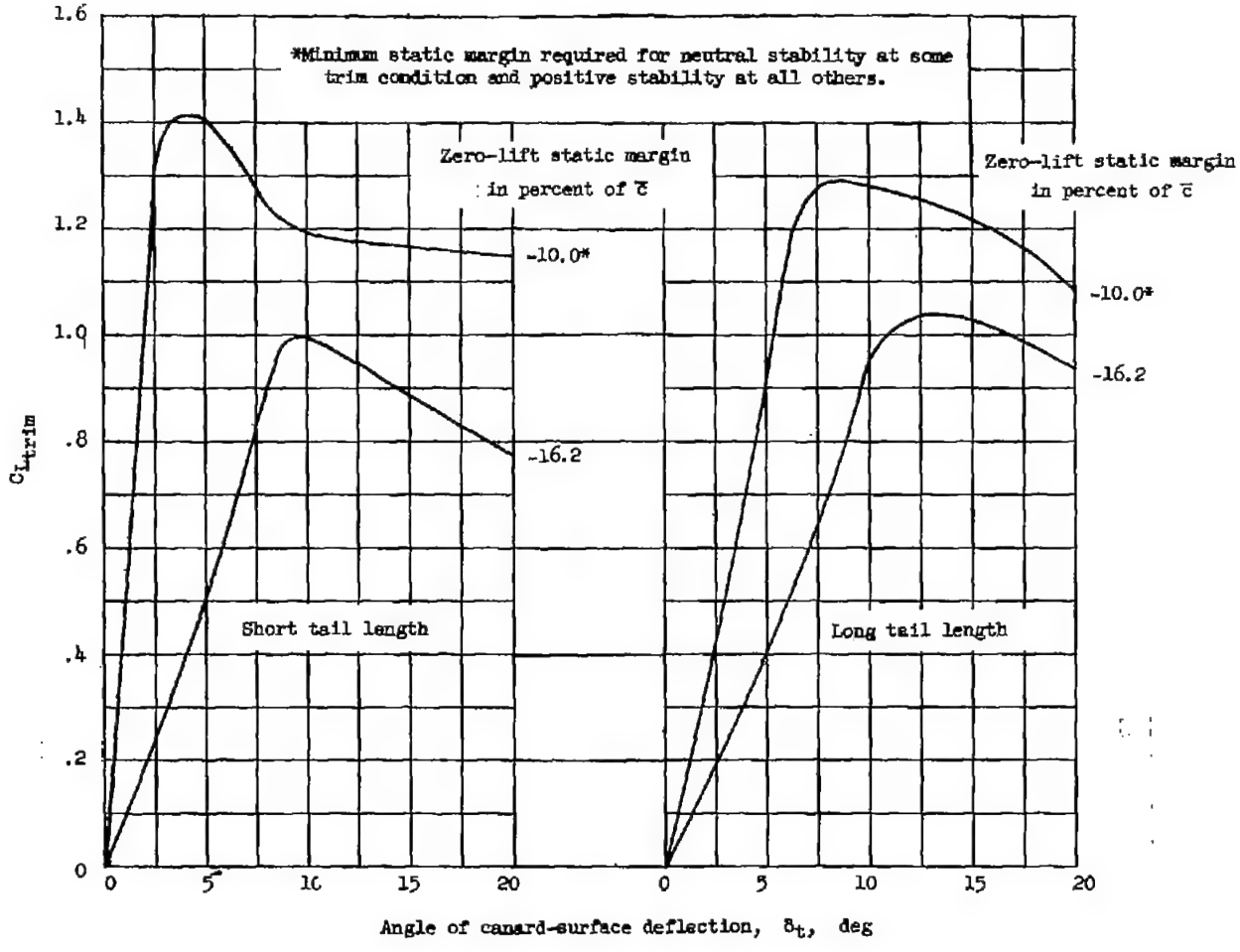

Figure 4.- Variation of trim lift coefficient with canard-surface deflection angle for two values of static margin and two longitudinal locations of the canard surface on a configuration having a wing and horizontal canard surface of 60° delta plan form.

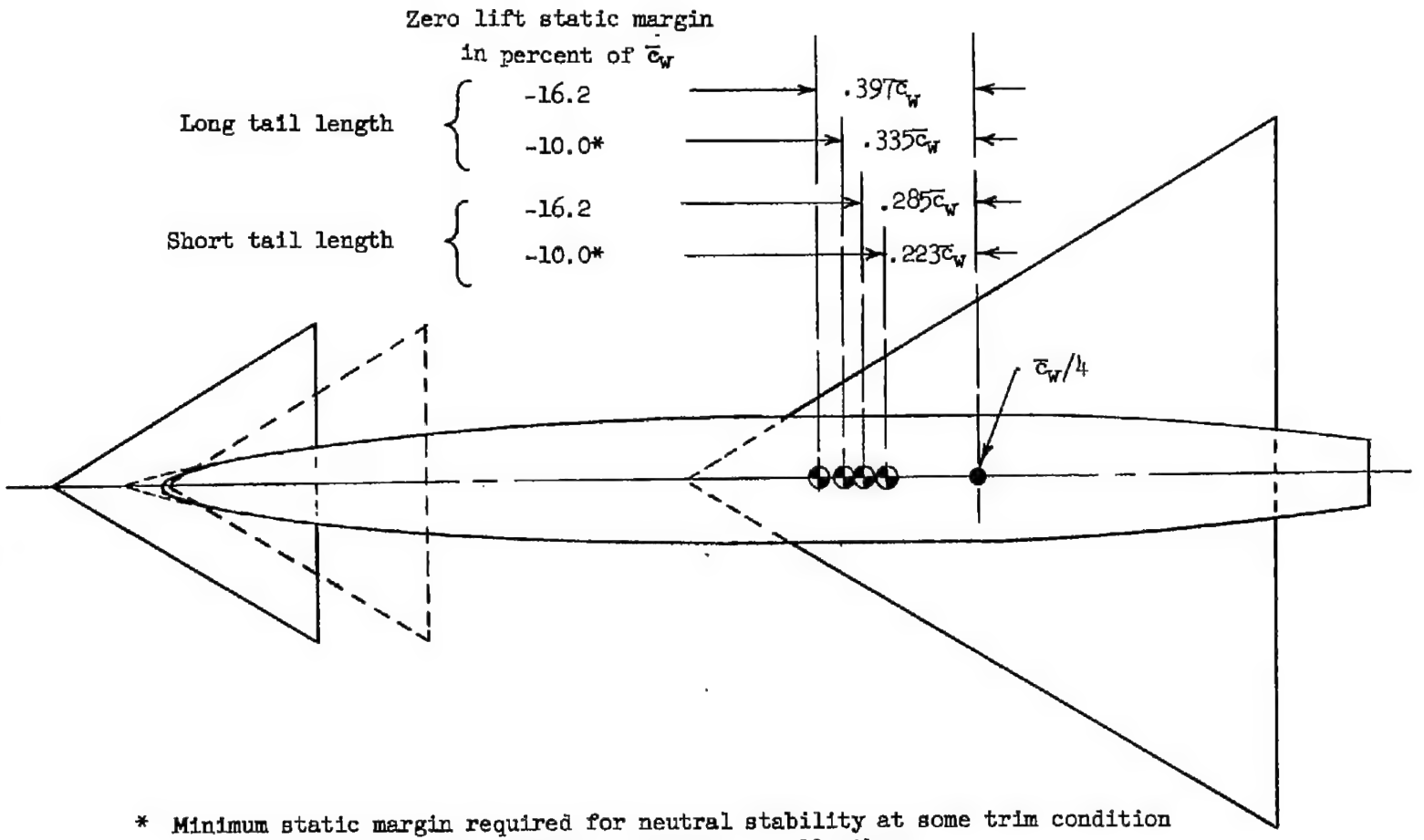

* Minimum static margin required for neutral stability at some trim condition and positive stability at all others

Figure 5.- Center-of-gravity positions for two values of static margin and two longitudinal positions of the canard surface on a configuration having a wing and horizontal canard surface of 60° delta plan form.

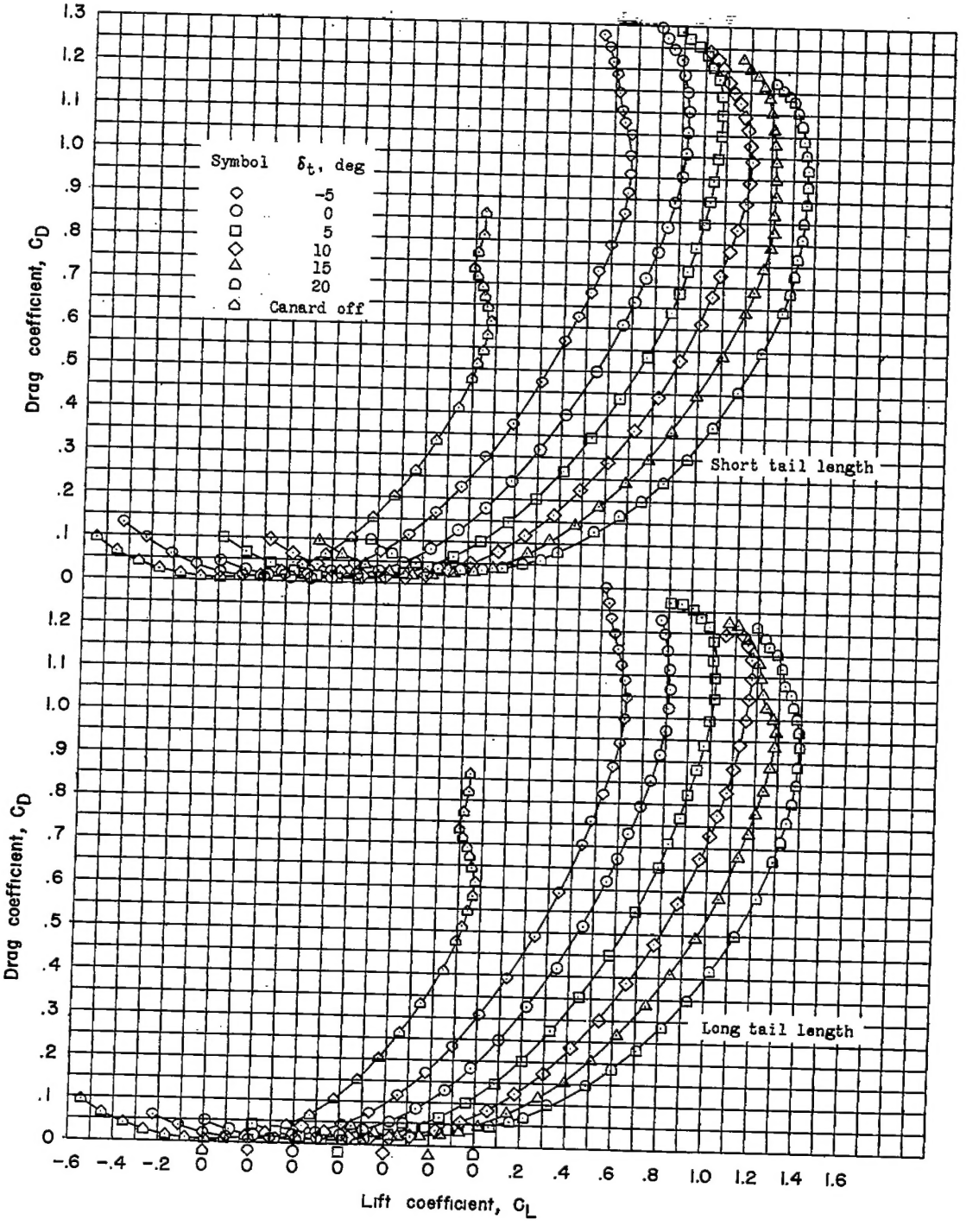

(a) Complete lift range.

Figure 6.- Variation of drag coefficient with lift coefficient for a configuration having a wing and horizontal canard surface of 60° delta plan form.

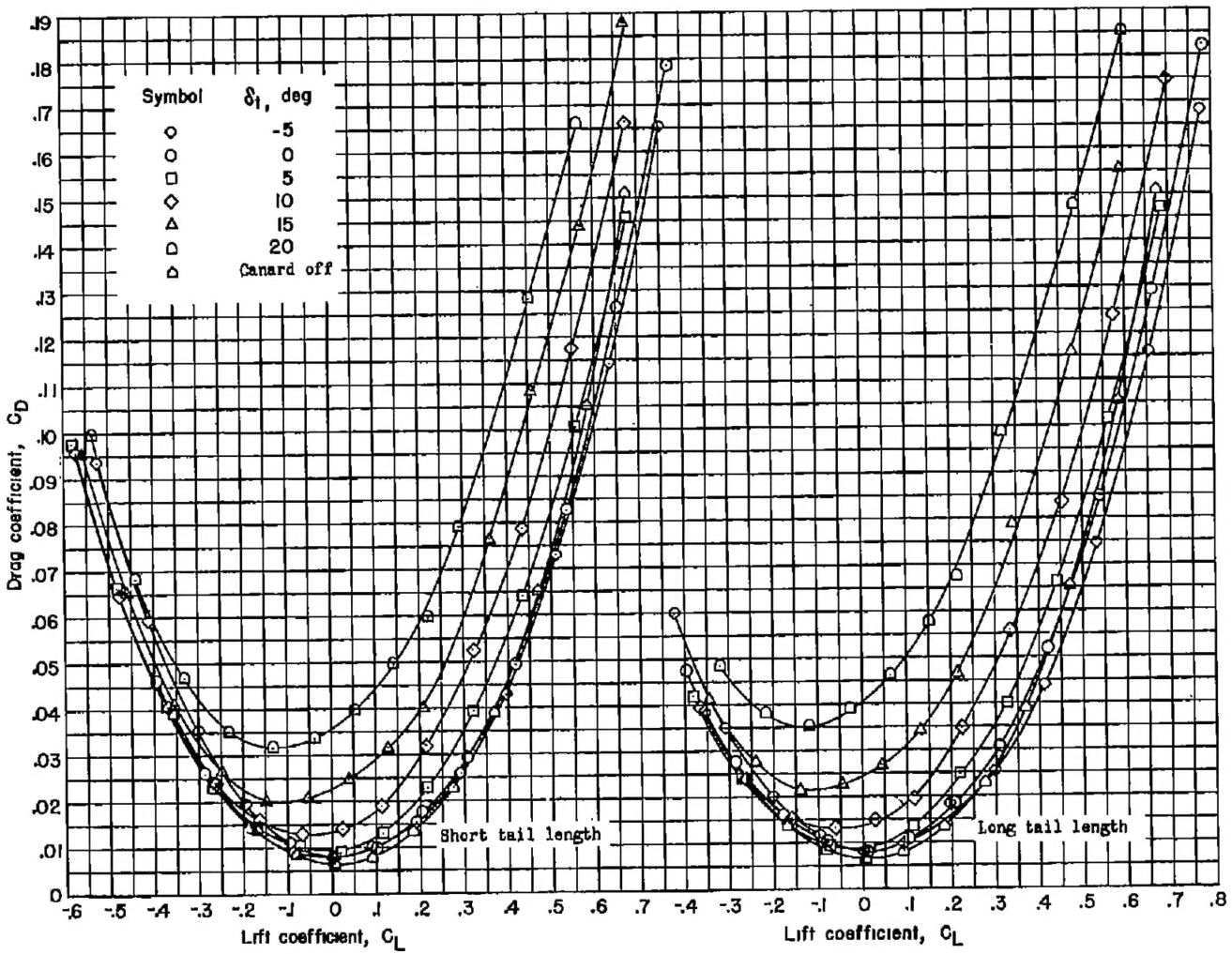

(b) Low lift range.

Figure 6.- Concluded.

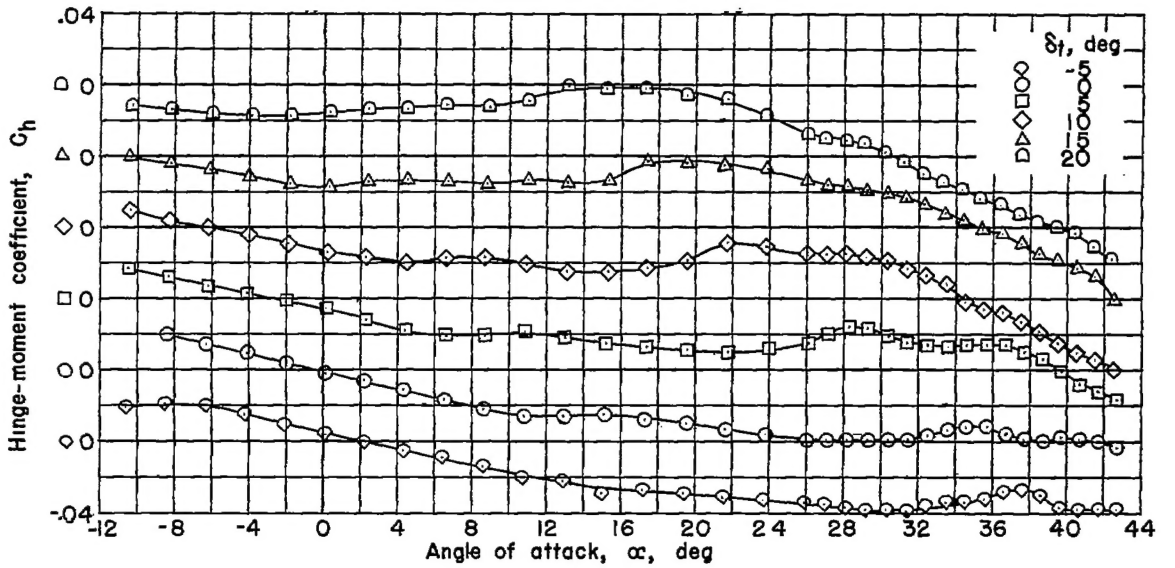

(a) Short tail length.

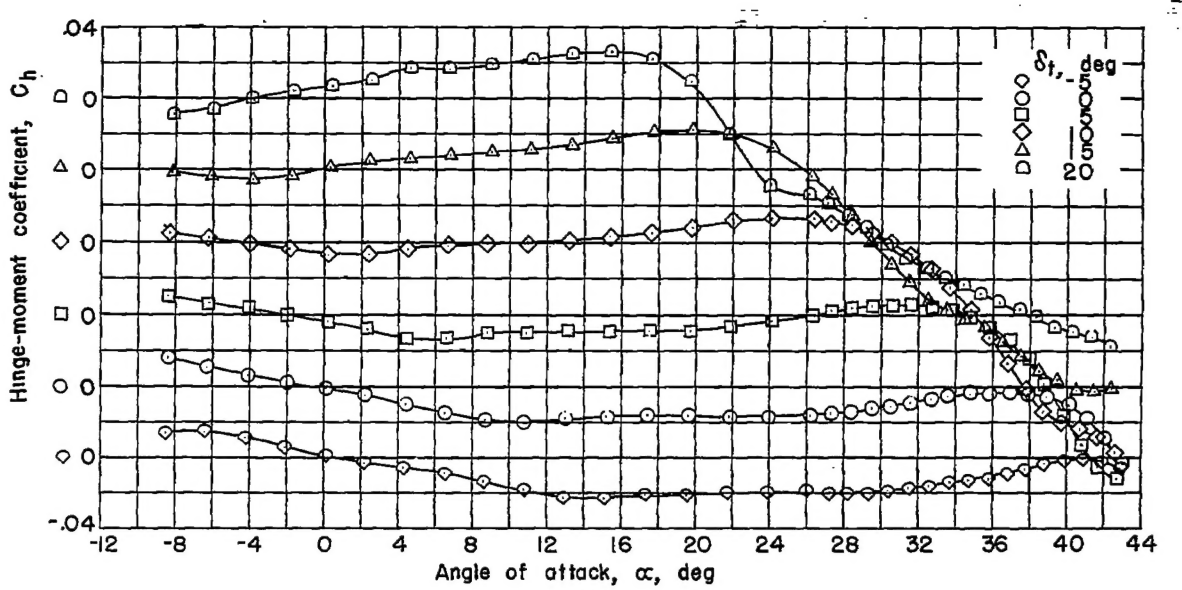

(b) Long tail length.

Figure 7.- Variation of canard-surface hinge-moment coefficient with angle of attack for a configuration having a wing and horizontal canard surface of 60° delta plan form.

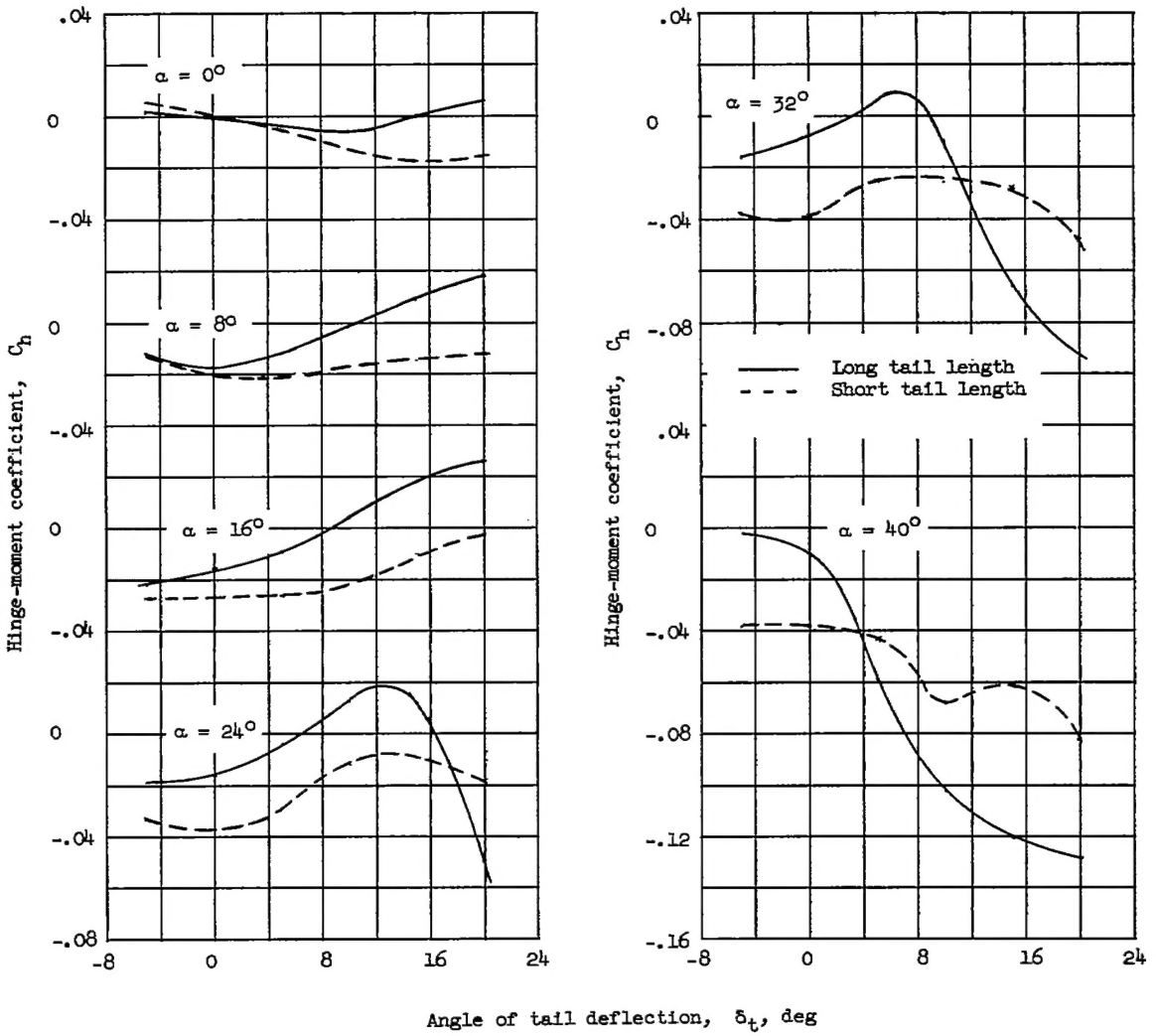

Figure 8.- Variation of canard-surface hinge-moment coefficient with deflection angle for a configuration having a wing and horizontal canard surface of 60° delta plan form.

[redacted]